Acta Mech 231, 4803–4818 (2020)
https://doi.org/10.1007/s00707-020-02797-2

ORIGINAL PAPER

M. H. B. M. Shariff · R. Bustamante

A spectral approach for nonlinear transversely isotropic elastic bodies, for a new class of constitutive equation: Applications to rock mechanics

Received: 30 April 2020 / Revised: 11 July 2020 / Accepted: 9 August 2020 / Published online: 28 August 2020

Abstract A constitutive equation is provided for nonlinear transversely isotropic elastic solids, wherein the linearized strain tensor is assumed to be a function of the Cauchy stress tensor; this elastic constitutive equation belongs to a subclass of a more general set of implicit constitutive relations proposed in the recent years. The proposed constitutive equation is valid for both compressible and incompressible bodies and can be simply modified, to exclude the mechanical influence of compressed fibres and to model inextensible fibres. A crude specific constitutive model is proposed to compare with a uniaxial experimental data on Marcellus shale. Some simple boundary value problems are analyzed.

1 Introduction

In recent years, some new constitutive equations and relations have been proposed for elastic [1–5] and inelastic bodies [6,7], where in general it is not assumed that the stresses are functions of the strains. One of such relatively new types of constitutive equation corresponds to the class wherein we have that the linearized strain tensor $\boldsymbol{\varepsilon}$ (infinitesimal strain tensor) is given as a function of the Cauchy stress tensor $\boldsymbol{T}$, i.e. $\boldsymbol{\varepsilon} = \mathfrak{h}(\boldsymbol{T})$ (see, for example, [8–12]). A subclass of the above equation is when we assume that there exists a scalar potential $\Pi = \Pi(\boldsymbol{T})$ such that (see [10]) $\mathfrak{h} = \frac{\partial \Pi}{\partial \boldsymbol{T}}$. The above constitutive equation $\boldsymbol{\varepsilon} = \frac{\partial \Pi}{\partial \boldsymbol{T}}$ has many potential applications, where we can observe a nonlinear behaviour for a solid when the strains and rotations are very small. Applications can be found, for example, in the mathematical modelling of the mechanical behaviour of concrete [13], some metal alloys [14,15], rock [16], fracture mechanics [17,18], and in the study of fibre-reinforced bodies [19].

With the exception of [19], in most of the works published on this type of constitutive equation so far, only isotropic bodies have been studied (see, for example, [20]). But there are many potential applications for $\boldsymbol{\varepsilon} = \frac{\partial \Pi}{\partial \boldsymbol{T}}$, where Π is a potential function for a transversely isotropic solid. For example, in [19] a model of inextensible bodies in a preferred direction was studied, for a matrix filled with a family of fibres, where it was very easy to model inextensibility in the direction of the fibres. In the case of the modelling of the mechanical behaviour of rocks, from the different literature available (see the short review at the beginning of Sect. 5), it is well known that many types of rocks are anisotropic, such as some metamorphic rocks like shale, schist, slates and gneiss, and sedimentary rocks such as sandstone and shales. Anisotropy of rocks can also appear as a product of the presence of micro-cracks, cracks, joints, bedding, and stratification[1].

[1] See, for example, [21–26], Table 1 of [27], [28–36], Figures 2-8, 4-10, 4-13 and 4-14 of [37], and [38,39].

M.H.B.M. Shariff
Department of Mathematics, Khalifa University of Science and Technology, Sharjah, UAE

R. Bustamante (✉)
Departamento de Ingeniería Mecánica, Universidad de Chile, Beauchef 851, Santiago Centro, Santiago, Chile
E-mail: rogbusta@ing.uchile.cl

In this paper, we present a constitutive equation based on $\boldsymbol{\varepsilon} = \frac{\partial \Pi}{\partial \boldsymbol{T}}$, where Π depends on $\boldsymbol{T}$ and $\boldsymbol{a} \otimes \boldsymbol{a}$, and where $\boldsymbol{a}$ is a unit vector in the preferred direction. We use spectral invariants, similar to that developed by Shariff [40], for the arguments of the function Π. Each spectral invariant has a clear interpretation, and invariants that have a clear meaningful physical interpretation are useful in assisting the construction of an experiment to seek a specific form of the potential function Π. We present a general model (that can be particularly useful for rocks) that contains single-variable functions which are easier to analyse than multivariable functions, and it can be easily amended (as shown later in this paper) to fully exclude the mechanical influence of compressed fibres and to model inextensible fibres. Our nonlinear expression for Π is constructed using the well-known Π expression for transversely isotropic linearized elastic bodies; in view of this, the proposed nonlinear model is consistent with the linear model, an important property that should be satisfied by a proper nonlinear model. We apply the above model to study the mechanical behaviour of a class of transversely isotropic rocks.

Considering the objectives of this paper discussed previously, this work is divided into the following Sections: In Sect. 2, some basic equations pertaining to the theory of elasticity are presented. In Sect. 3, general expressions for Π are developed using spectral invariants. In Sect. 4, some boundary value problems are studied for cylinders and a slab considering homogeneous distributions of stresses and strains. In Sect. 5, particular expressions are given for the constitutive equations in the case of modelling the mechanical behaviour of Marcellus shale. In Sect. 6, some final remarks are given.

2 Kinematics and equation of motion

In this paper, summation convention is not used, and all subscripts i, j and k take the values 1, 2, 3, unless stated otherwise.

A particle in a body $\mathscr{B}$ is denoted by X, and in the reference configuration $\boldsymbol{\kappa}_R(\mathscr{B})$, the particle X occupies the position $\boldsymbol{X} = \boldsymbol{\kappa}_R(X)$. In the current configuration $\boldsymbol{\kappa}_t(\mathscr{B})$, the position of a point X is denoted by $\boldsymbol{x}$, and it is assumed that there exists a one-to-one mapping $\boldsymbol{\chi}$ such that $\boldsymbol{x} = \boldsymbol{\chi}(\boldsymbol{X}, t)$. The deformation gradient, the left Cauchy–Green tensor, and the displacement vector are defined as

$$\boldsymbol{F} = \frac{\partial \boldsymbol{\chi}}{\partial \boldsymbol{X}}, \quad \boldsymbol{B} = \boldsymbol{F}\boldsymbol{F}^{\mathrm{T}} = \boldsymbol{V}^2, \quad \boldsymbol{u} = \boldsymbol{x} - \boldsymbol{X}, \tag{1}$$

where $\boldsymbol{V}$ is the left stretch tensor. In infinitesimal strain deformation, the current and reference configurations are indistinguishable, and we have

$$\boldsymbol{B} - \boldsymbol{I} \approx 2\boldsymbol{\varepsilon}\,, \tag{2}$$

where $\boldsymbol{I}$ is the identity tensor, $\boldsymbol{\varepsilon}$ is the infinitesimal strain tensor defined as

$$\boldsymbol{\varepsilon} = \frac{1}{2}[\operatorname{grad}\boldsymbol{u} + (\operatorname{grad}\boldsymbol{u})^{\mathrm{T}}]\,, \tag{3}$$

and grad is the gradient operator with respect to $\boldsymbol{x}$.

We denote the Cauchy stress by $\boldsymbol{T}$, and the equation of motion takes the form

$$\rho\ddot{\boldsymbol{x}} = \operatorname{div}\boldsymbol{T} + \rho\boldsymbol{b}\,, \tag{4}$$

where div is the divergence of a tensor with respect to $\boldsymbol{x}$, ρ is the density of the body, and $\boldsymbol{b}$ represents the specific body forces. We use the notation $\dot{(\,)}$ for the time derivative. More details concerning the kinematics of deformable bodies and the balance equations can be found in [41].

3 Constitutive relations and equations

The constitutive equation to be used in this work has been presented in [8–10] and is a subclass of the implicit relation $\mathfrak{G}(\boldsymbol{T}, \boldsymbol{B}) = \boldsymbol{0}$, which was proposed by Rajagopal [2] for elastic bodies (see also [42]). Two special subclasses of the above implicit relation are the classical Cauchy model, wherein the stress is assumed to be a function of the strains (see [43]) $\boldsymbol{T} = \mathfrak{F}(\boldsymbol{B})$, and the new class $\boldsymbol{B} = \mathfrak{H}(\boldsymbol{T})$. There is another class of model that is similar to $\boldsymbol{B} = \mathfrak{H}(\boldsymbol{T})$, which is based on the use of the Hencky's logarithmic strain $\frac{1}{2}\ln\boldsymbol{B}$ as a function

of the Kirchhoff stress $\boldsymbol{\tau} = J\boldsymbol{T}$, i.e. $\frac{1}{2}\ln \boldsymbol{B} = \mathfrak{g}(\boldsymbol{\tau})$. That model has been studied, for example, in [44–47] (see also the early work by Blume [48] on such inverted stress–strain constitutive equations).

In this case, we assume that the gradient of the displacement field is very small $|\mathrm{grad}\,\boldsymbol{u}| \sim O(\delta)$, $\delta \ll 1$, from $\mathfrak{G}(\boldsymbol{T}, \boldsymbol{B}) = \boldsymbol{0}$ or the subclasses of constitutive equations $\boldsymbol{B} = \mathfrak{H}(\boldsymbol{T})$, $\frac{1}{2}\ln \boldsymbol{B} = \mathfrak{g}(\boldsymbol{\tau})$; in view of (2), it is possible to obtain $\boldsymbol{\varepsilon} = \mathfrak{h}(\boldsymbol{T})$, where we observe that the linearized strain is a function of the stresses. Such constitutive equation, for example, has been used to study problems in rock and concrete [13,16]. In this paper, we consider rock as elastic and assume the existence of a scalar function (see [10])

$$\Pi = \Pi_{(T)} = \Pi_{(e)}(\boldsymbol{T}, \boldsymbol{a}\otimes\boldsymbol{a}) = \Pi_{(e)}\left(\boldsymbol{Q}\boldsymbol{T}\boldsymbol{Q}^T, \boldsymbol{Q}\boldsymbol{a}\otimes\boldsymbol{a}\boldsymbol{Q}^T\right) \tag{5}$$

such that

$$\boldsymbol{\varepsilon} = \frac{\partial \Pi_{(T)}}{\partial \boldsymbol{T}}\,. \tag{6}$$

The potential $\Pi_{(T)}$ can be identified as the Gibbs potential in the case the gradient of the displacement field is very small (see, for example, [46,47]).

In some materials, there is some experimental evidence (see, for example, the work of Jin et al. [49]), which indicates that the values of the ground-state constants in hydrostatic compression are different from those in hydrostatic tension[2]. In view of this, we assume that the ground-state constants depend on the spherical stress

$$\bar{h} = \frac{1}{3}\mathrm{tr}\,\boldsymbol{T}\,. \tag{7}$$

Hence, we suppose the values of the five independent ground-state constants for the linearized elastic model ν_a, ν_p, E_p, E_a, and μ_a when $\bar{h} < 0$ are generally different from those when $\bar{h} \geq 0$ (see 'Appendix A'). Here, ν_p is Poisson's ratio in a particular direction on the plane of symmetry, when the material is extended in a direction on the plane of symmetry perpendicular to the particular direction, ν_a is Poisson's ratio in the preferred direction when the material is extended in the plane of symmetry, E_p is Young's Modulus in the plane of symmetry normal to the preferred direction $\boldsymbol{a}$, μ_a is the shear modulus in the preferred direction, and E_a is Young's modulus in the preferred direction. Take note that we also have the relation

$$\frac{\nu_a}{E_p} = \frac{\nu_{zp}}{E_a}\,, \tag{8}$$

where ν_{zp} is Poisson's ratio in any direction on the plane of symmetry, when the material is extended in the preferred direction.

Following the work of Shariff [50], we can express $\Pi_{(T)}$ in terms of the spectral invariants

$$\sigma_i(\boldsymbol{T}) = \sigma_i(\boldsymbol{Q}\boldsymbol{T}\boldsymbol{Q}^T) = \boldsymbol{v}_i\cdot(\boldsymbol{T}\boldsymbol{v}_i)\,,\quad \zeta_i = (\boldsymbol{v}_i\cdot\boldsymbol{a})^2 = [(\boldsymbol{Q}\boldsymbol{v}_i)\cdot(\boldsymbol{Q}\boldsymbol{a})]^2\,, \tag{9}$$

where σ_i and $\boldsymbol{v}_i$ are the principal stresses and principal directions of $\boldsymbol{T}$,

$$\boldsymbol{T} = \sum_{i=1}^{3}\sigma_i\,\boldsymbol{v}_i\otimes\boldsymbol{v}_i\,,\quad \mathrm{tr}\,\boldsymbol{T} = \sum_{i=1}^{3}\sigma_i\,. \tag{10}$$

Only five of the six spectral invariants in (9) are independent since we have the constraint

$$\zeta_1 + \zeta_2 + \zeta_3 = 1\,. \tag{11}$$

In Sect. 3.1, we review briefly the expression for $\Pi_{(T)}$ that is used in the linearized theory of elasticity, and the structure of that function is used, in Sect. 3.2, as starting point for the development of a nonlinear model for $\Pi_{(T)}$.

[2] By the ground-state constants, we mean the material constants used for the linearized elastic models.

3.1 Linearized strain–stress constitutive equation

Let us define the scale stress $\hat{\boldsymbol{T}} = \dfrac{1}{E_p}\boldsymbol{T}$; hence, for $|\hat{\sigma}_i| = \left|\dfrac{\sigma_i}{E_p}\right| << 1$, the most general quadratic form, satisfying $\Pi_{(T)} = 0$ and $\dfrac{\partial \Pi_{(T)}}{\partial \boldsymbol{T}} = \boldsymbol{0}$ at $\boldsymbol{T} = \boldsymbol{0}$, is:

$$\Pi_{(T)} = c_1 E_p^2 \left[\sum_{i=1}^{3} \hat{\sigma_i}^2 + c_2 \left(\sum_{i=1}^{3} \hat{\sigma}_i \right)^2 + c_3 \sum_{i=1}^{3} \zeta_i \hat{\sigma_i}^2 + c_4 \left(\sum_{i=1}^{3} \zeta_i \hat{\sigma}_i \right)^2 + c_5 \left(\sum_{i=1}^{3} \zeta_i \hat{\sigma}_i \right) \left(\sum_{i=1}^{3} \hat{\sigma}_i \right) \right], \tag{12}$$

$$= c_1 \sum_{i=1}^{3} \sigma_i^2 + c_2 \left(\sum_{i=1}^{3} \sigma_i \right)^2 + c_3 \sum_{i=1}^{3} \zeta_i \sigma_i^2 + c_4 \left(\sum_{i=1}^{3} \zeta_i \sigma_i \right)^2 + c_5 \left(\sum_{i=1}^{3} \zeta_i \sigma_i \right) \left(\sum_{i=1}^{3} \sigma_i \right), \tag{13}$$

where the constants c_k, $k = 1, 2, 3, 4, 5$ are defined as

$$c_1 = \frac{1+\nu_p}{2E_p}, \quad c_2 = -\frac{\nu_p}{2E_p}, \quad c_3 = \frac{1}{4\mu_a} - \frac{1+\nu_p}{2E_p}, \quad c_4 = \frac{1}{2E_a} + \frac{2\nu_a - \nu_p}{2E_p} - \frac{1}{4\mu_a}, \quad c_5 = \frac{\nu_p - \nu_a}{E_p}. \tag{14}$$

Let us express the above scalar function in the form

$$\frac{\Pi_{(T)}}{E_p^2} = \left[b_1 \sum_{i=1}^{3} \bar{\sigma}_i^{*2} + b_2 h^2 + b_3 \sum_{i=1}^{3} \zeta_i \bar{\sigma}_i^{*2} + b_4 \left(\sum_{i=1}^{3} \zeta_i \bar{\sigma}_i^* \right)^2 + b_5 h \sum_{i=1}^{3} \zeta_i \bar{\sigma}_i^* \right], \tag{15}$$

where

$$h = \frac{1}{E_p} \mathrm{tr}\, \boldsymbol{T}, \quad \bar{\sigma}_i^* = \hat{\sigma}_i - \frac{h}{3} \tag{16}$$

and

$$b_1 = c_1, \quad b_2 = \frac{c_1}{3} + c_2 + \frac{c_3}{9} + \frac{c_4}{9} + \frac{c_5}{3}, \quad b_3 = c_3, \quad b_4 = c_4, \quad b_5 = \frac{2}{3}(c_3 + c_4) + c_5. \tag{17}$$

Note that only five of the seven invariants

$$h = \frac{1}{E_p} \mathrm{tr}\, \boldsymbol{T} = \frac{1}{E_p} \mathrm{tr}(\boldsymbol{Q}\boldsymbol{T}\boldsymbol{Q}^T), \quad \bar{\sigma}_i^*(\boldsymbol{T}) = \bar{\sigma}_i^*(\boldsymbol{Q}\boldsymbol{T}\boldsymbol{Q}^T), \quad \zeta_i \tag{18}$$

characterizing the scalar function (12), are independent due to the constraints (11), and

$$\bar{\sigma}_1^* + \bar{\sigma}_2^* + \bar{\sigma}_3^* = 0. \tag{19}$$

The strain–stress constitutive equation is given by

$$\boldsymbol{\varepsilon} = \frac{\partial \Pi_{(T)}}{\partial \boldsymbol{T}} = 2b_1 \bar{\boldsymbol{T}}^* + 2b_2 h \boldsymbol{I} + b_3 \left[\boldsymbol{A}\bar{\boldsymbol{T}}^* + \bar{\boldsymbol{T}}^* \boldsymbol{A} - \frac{2}{3} \mathrm{tr}(\boldsymbol{A}\bar{\boldsymbol{T}}^*) \boldsymbol{I} \right] + 2b_4 \mathrm{tr}(\boldsymbol{A}\bar{\boldsymbol{T}}^*) \left[\boldsymbol{A} - \frac{1}{3}\boldsymbol{I} \right] + b_5 \left[\left(\boldsymbol{A} - \frac{1}{3}\boldsymbol{I} \right) h + \mathrm{tr}(\boldsymbol{A}\bar{\boldsymbol{T}}^*) \boldsymbol{I} \right], \tag{20}$$

where $\boldsymbol{A} = \boldsymbol{a} \otimes \boldsymbol{a}$ and

$$\bar{\boldsymbol{T}}^* = \hat{\boldsymbol{T}} - \frac{h}{3}\boldsymbol{I}\,. \tag{21}$$

The volume change is

$$\mathrm{tr}\,\boldsymbol{\varepsilon} = 6b_2 h + 3b_5 \mathrm{tr}\,(\boldsymbol{A}\bar{\boldsymbol{T}}^*)\,. \tag{22}$$

When the body is incompressible, $\nu_{zp} = 0.5$ and $1 - \nu_a - \nu_p = 0$, in view of (14) and (17), we have $b_2 = b_5 = 0$, and hence,

$$\mathrm{tr}\,\boldsymbol{\varepsilon} = 0\,. \tag{23}$$

3.2 Nonlinear strain–stress constitutive equation

Using the quadratic function Π in (13) as inspiration or starting point, we propose the non-quadratic function

$$\frac{\Pi_{(T)}}{E_p^2} = b_1 K_0 + b_2 g_0(h) + b_3 K_1 + b_4 K_2^2 + b_5 K_3 g_1(h)\,, \tag{24}$$

where

$$K_0 = \sum_{i=1} f_0(\bar{\sigma}_i^*)\,, \tag{25}$$

and

$$K_\alpha = \sum_{i=1}^{3} \zeta_i\, f_\alpha(\bar{\sigma}_i^*)\,, \quad \alpha = 1, 2, 3\,. \tag{26}$$

In order to be consistent with the linearized model (12), we impose the conditions

$$\begin{aligned} &f_0(0) = f_0'(0) = g_0'(0) = f_1(0) = f_1'(1) = 0\,, \quad f_0''(0) = g_0''(0) = f_1''(0) = 2\,, \\ &f_\beta(0) = g_1(0) = 0\,, \quad f_\beta'(0) = g_1'(0) = 1\,, \beta = 2, 3\,. \end{aligned} \tag{27}$$

We also impose the conditions $f_0, g_0, f_1 \geq 0$, f_0', g_0', f_1' are strict monotonic functions, i.e. $f_0'', g_0'', f_1'' > 0$, and $f_0'(x), g_0'(x), f_1'(x) > 0$ and $f_0'(x), g_0'(x), f_1'(x) < 0$ for $x > 0$ and $x < 0$, respectively. The functions f_β, g_1 ($\beta = 2, 3$) are strictly monotone, i.e. $f_\beta', g_1' > 0$. Note that $\Pi_{(T)}$ must satisfy the P-property (see [51]), i.e. that it has a unique value when two or more of the $\bar{\sigma}_i^*$ have the same value and it satisfies the symmetric property described below,

$$\begin{aligned} \Pi_{(T)} &= \Pi_t(\bar{\sigma}_1^*, \bar{\sigma}_2^*, \bar{\sigma}_3^*, \zeta_1, \zeta_2, \zeta_3) = \Pi_t(\bar{\sigma}_2^*, \bar{\sigma}_1^*, \bar{\sigma}_3^*, \zeta_2, \zeta_1, \zeta_3) \\ &= \Pi_t(\bar{\sigma}_1^*, \bar{\sigma}_3^*, \bar{\sigma}_2^*, \zeta_1, \zeta_3, \zeta_2) = \Pi_t(\bar{\sigma}_3^*, \bar{\sigma}_2^*, \bar{\sigma}_1^*, \zeta_3, \zeta_2, \zeta_1)\,. \end{aligned} \tag{28}$$

The infinitesimal strain is given by

$$\boldsymbol{\varepsilon} = \sum_{i,j=1}^{3} \left(\frac{\partial \Pi_{(T)}}{\partial \boldsymbol{T}}\right)_{ij} \boldsymbol{v}_i \otimes \boldsymbol{v}_j\,, \tag{29}$$

where, following the work of Shariff [52], we have

$$\left(\frac{\partial \Pi_{(T)}}{\partial \boldsymbol{T}}\right)_{ii} = \frac{\partial \Pi_t}{\partial \sigma_i}\,, \tag{30}$$

$$\left(\frac{\partial \Pi_{(T)}}{\partial \boldsymbol{T}}\right)_{ij} = \frac{a_i a_j}{(\sigma_i - \sigma_j)}\left(\frac{\partial \Pi_t}{\partial \zeta_i} - \frac{\partial \Pi_t}{\partial \zeta_j}\right) \quad i \neq j\,, \tag{31}$$

where $a_i = \boldsymbol{v}_i \cdot \boldsymbol{a}$.

In view of the results

$$E_p \frac{\partial K_0}{\partial \boldsymbol{T}} = \sum_{i=1}^{3} f_0'(\bar{\sigma}_i^*) \left(\boldsymbol{v}_i \otimes \boldsymbol{v}_i - \frac{1}{3}\boldsymbol{I} \right), \quad E_p \frac{\partial g_\alpha}{\partial \boldsymbol{T}} = g_\alpha'(h)\boldsymbol{I}, \quad \alpha = 0, 1, \tag{32}$$

$$E_p \frac{\partial K_\alpha}{\partial \boldsymbol{T}} = \sum_{i=1}^{3} \zeta_i f_\alpha'(\bar{\sigma}_i^*) \left(\boldsymbol{v}_i \otimes \boldsymbol{v}_i - \frac{1}{3}\boldsymbol{I} \right) + \sum_{i \neq j=}^{3} \frac{f_\alpha(\bar{\sigma}_i^*) - f_\alpha(\bar{\sigma}_j^*)}{\bar{\sigma}_i^* - \bar{\sigma}_j^*} a_i a_j \boldsymbol{v}_i \otimes \boldsymbol{v}_j ,$$
$$\alpha = 1, 2, 3, \tag{33}$$

we have the volume change,

$$\operatorname{tr} \boldsymbol{\varepsilon} = 3b_2 g_0'(h) + 3b_5 K_3 g_1'(h). \tag{34}$$

If $b_2 = b_5 = 0$, we have $\operatorname{tr} \boldsymbol{\varepsilon} = 0$, and in such a situation, we can model the behaviour of an incompressible body.

We also show that the proposed constitutive equation can be easily converted to allow the mechanical influence of compressed fibres to be excluded and to model a body that is inextensible in the preferred direction $\boldsymbol{a}$. In the case when the influence of compressed fibres is negligible, we have

$$E_a = E_p, \quad \nu_a = \nu_{zp} = \nu_p, \quad E_p = 2\mu_a(1 + \nu_a), \tag{35}$$

and hence,

$$c_3 = c_4 = c_5 = b_3 = b_4 = b_5 = 0. \tag{36}$$

We note that

$$\varphi = \boldsymbol{a} \cdot (\boldsymbol{\varepsilon}\boldsymbol{a}) = \sum_{m=1}^{5} b_m \psi_m , \tag{37}$$

where

$$\psi_1 = \sum_{i=1}^{3} f_0'(\bar{\sigma}_i^*) \left(\zeta_i - \frac{1}{3} \right), \quad \psi_2 = g_0'(h), \tag{38}$$

$$\psi_3 = \sum_{i=1}^{3} f_1'(\bar{\sigma}_i^*) \zeta_i \left(\zeta_i - \frac{1}{3} \right) + \sum_{i \neq j=1} \frac{f_1(\bar{\sigma}_i^*) - f_1(\bar{\sigma}_j^*)}{\bar{\sigma}_i^* - \bar{\sigma}_j^*} \zeta_i \zeta_j , \tag{39}$$

$$\psi_4 = 2I_2 \sum_{i=1}^{3} f_2'(\bar{\sigma}_i^*) \zeta_i \left(\zeta_i - \frac{1}{3} \right) + \sum_{i \neq j=1} \frac{f_2(\bar{\sigma}_i^*) - f_2(\bar{\sigma}_j^*)}{\bar{\sigma}_i^* - \bar{\sigma}_j^*} \zeta_i \zeta_j , \tag{40}$$

$$\psi_5 = g_1(h) \sum_{i=1}^{3} f_3'(\bar{\sigma}_i^*) \zeta_i \left(\zeta_i - \frac{1}{3} \right) + \sum_{i \neq j=1} \frac{f_3(\bar{\sigma}_i^*) - f_3(\bar{\sigma}_j^*)}{\bar{\sigma}_i^* - \bar{\sigma}_j^*} \zeta_i \zeta_j + K_3 g_1'(h). \tag{41}$$

To take into account that the influence of compressed fibres is negligible, we can easily modify our constitutive equation (24) by using a function $q_{(p)}$, given in Appendix A, where the modified scalar potential takes the form

$$\frac{\Pi_{(T)}}{E_p^2} = b_1 K_0 + b_2 g_0(h) + q_{(p)}(\varphi)[b_3 K_1 + b_4 K_2^2 + b_5 K_3 g_1(h)], \tag{42}$$

taking note that when a fibre is in compression, we have $\varphi < 0$ and $q_{(p)}(\varphi) = 0$.

When the fibres are inextensible, $\varphi = 0$, and (42) is replaced by

$$\frac{\Pi_{(T)}}{E_p^2} = b_1 K_0 + b_2 g_0(h) + q_{(p)}(\varphi)[b_3 K_1 + b_4 K_2^2 + b_5 K_3 g_1(h) + \hat{\lambda}\varphi], \tag{43}$$

where $\hat{\lambda}$ is a Lagrange multiplier. The strain is given by

$$\frac{\boldsymbol{\varepsilon}}{E_p^2} = b_1\frac{\partial K_0}{\partial \boldsymbol{T}} + b_2\frac{\partial g_0}{\partial \boldsymbol{T}} + q_{(p)}(\varphi)\left\{b_3\frac{\partial K_1}{\partial \boldsymbol{T}} + 2b_4K_2\frac{\partial K_2}{\partial \boldsymbol{T}} + b_5\left[g_1(h)\frac{\partial K_3}{\partial \boldsymbol{T}} + K_3\frac{\partial g_1}{\partial \boldsymbol{T}}\right] + \bar{\lambda}\frac{\partial \varphi}{\partial \boldsymbol{T}}\right\}, \quad (44)$$

where it is emphasized that, for practical purposes, we let the value of the derivative of $q_{(p)}$ be zero.

The nonlinear model presented in this Section can be used not only to model rock, as studied in detail in Sect. 5, but to model nonlinear behaviour of small strains and rotations of any transversely isotropic elastic material.

4 Homogeneous boundary value problems

In the problems presented in this Section we assume homogeneous time-independent distributions for the stresses and strains, which automatically satisfy the equilibrium and compatibility equations.

4.1 Cylindrical axial deformation

Consider a cylinder with the configuration

$$0 \le r \le A\,, \quad 0 \le \theta \le 2\pi\,, \quad 0 \le z \le L\,, \quad (45)$$

and the case $\boldsymbol{a} = \boldsymbol{e}_z$ with the Cauchy stress having the form

$$\boldsymbol{T} = \sigma_r \boldsymbol{e}_r \otimes \boldsymbol{e}_r + \sigma_\theta \boldsymbol{e}_\theta \otimes \boldsymbol{e}_\theta + \sigma_z \boldsymbol{e}_z \otimes \boldsymbol{e}_z\,, \quad (46)$$

where $\boldsymbol{v}_1 = \boldsymbol{e}_r$, $\boldsymbol{v}_2 = \boldsymbol{e}_\theta$, and $\boldsymbol{v}_3 = \boldsymbol{e}_z$. In this case, we have $\zeta_3 = 1$ and $\zeta_1 = \zeta_2 = 0$, and clearly, from (31), we obtain $\varepsilon_{r\theta} = \varepsilon_{rz} = \varepsilon_{z\theta} = 0$, and hence the strain $\boldsymbol{\varepsilon}$ is coaxial with the Cauchy stress $\boldsymbol{T}$.

We first consider the case when $\sigma_r = \sigma_\theta = E_p\kappa$ and $\sigma_z = E_p\tau$, where κ and τ are dimensionless variables. Hence,

$$\bar{\sigma}_1^* = \bar{\sigma}_2^* = \frac{\tau - \kappa}{3} = \gamma = \frac{\bar{\sigma}_3^*}{2}\,. \quad (47)$$

The nonzero strain components take the forms

$$\begin{aligned}\varepsilon_{zz} &= \frac{2}{3}b_1[f_0'(2\gamma) - f_0'(-\gamma)] + b_2g_0'(h) + \frac{2}{3}b_3f_1'(2\gamma) + \frac{4}{3}b_4f_2(2\gamma)f_2'(2\gamma)\\ &\quad + b_5\left[\frac{2}{3}g_1(h)f_2'(2\gamma) + f_2(2\gamma)g_1'(h)\right], \quad (48)\\ \varepsilon_{rr} = \varepsilon_{\theta\theta} &= \frac{1}{3}b_1[f_0'(-\gamma) - f_0'(2\gamma)] + b_2g_0'(h) - \frac{1}{3}b_3f_1'(2\gamma) - \frac{2}{3}b_4f_2(2\gamma)f_2'(2\gamma)\\ &\quad + b_5\left[-\frac{1}{3}g_1(h)f_3'(2\gamma) + f_3(2\gamma)g_1'(h)\right]. \quad (49)\end{aligned}$$

When the lateral deformation is not constrained, $\sigma_r = \sigma_\theta = 0$ and $\sigma_z = E_p\tau$, and we use the value of $\gamma = -\frac{\tau}{3}$ for the different functions given in (48) and (49).

For the case when the lateral deformation is constrained such that $\varepsilon_{rr} = \varepsilon_{\theta\theta} = 0$, we have for $\sigma_z = E_p\tau$ that

$$E_p\bar{\sigma}_1^* = \frac{2\sigma_r}{3} - \frac{1}{3}(\sigma_\theta + E_p\tau)\,, \quad E_p\bar{\sigma}_2^* = \frac{2\sigma_\theta}{3} - \frac{1}{3}(\sigma_r + E_p\tau)\,, \quad E_p\bar{\sigma}_3^* = \frac{2E_p\tau}{3} - \frac{1}{3}(\sigma_r + \sigma_\theta)\,. \quad (50)$$

In view of the above, we have

$$\begin{aligned}\varepsilon_{rr} = 0 &= \frac{1}{3}b_1[2f_0'(\bar{\sigma}_1^*) - f_0'(\bar{\sigma}_2^*) - f_0'(\bar{\sigma}_3^*)] + b_2g_0'(h) - \frac{1}{3}b_3f_1'(\bar{\sigma}_3^*) - \frac{2}{3}b_4f_2(\bar{\sigma}_3^*)f_2'(\bar{\sigma}_3^*)\\ &\quad + b_5\left[-\frac{1}{3}g_1'(h)f_3'(\bar{\sigma}_3^*) + f_3(\bar{\sigma}_3^*)g_1'(h)\right] \quad (51)\end{aligned}$$

and

$$\varepsilon_{\theta\theta} = 0 = \frac{1}{3}b_1[2f_0'(\bar{\sigma}_2^*) - f_0'(\bar{\sigma}_1^*) - f_0'(\bar{\sigma}_3^*)] + b_2 g_0'(h) - \frac{1}{3}b_3 f_1'(\bar{\sigma}_3^*) - \frac{2}{3}b_4 f_2(\bar{\sigma}_3^*) f_2'(\bar{\sigma}_3^*) + b_5\left[-\frac{1}{3}g_1'(h) f_3'(\bar{\sigma}_3^*) + f_3(\bar{\sigma}_3^*) g_1'(h)\right]. \tag{52}$$

It is clear from (51) and (52) that

$$f_0'(\bar{\sigma}_1^*) = f_0'(\bar{\sigma}_2^*). \tag{53}$$

Since f_0' is a monotonic function, f_0' is invertible and (53) implies $\sigma_r = \sigma_\theta$, and they can be expressed in terms of τ in any of the two equations (51) or (52).

4.2 Compression and tension of a slab

Let x_i be the Cartesian coordinates with basis $\{\boldsymbol{g}_1, \boldsymbol{g}_2, \boldsymbol{g}_3\}$ and consider the configuration of a slab described by

$$-\frac{L_i}{2} \le x_i \le \frac{L_i}{2}. \tag{54}$$

In this Section, we consider the Cauchy stress to take the form

$$\boldsymbol{T} = \sum_{i=1} \sigma_i \boldsymbol{g}_i \otimes \boldsymbol{g}_i, \tag{55}$$

i.e. $\boldsymbol{v}_i = \boldsymbol{g}_i$, and we consider the preferred direction $\boldsymbol{a}$ to be given as

$$\boldsymbol{a} = s\boldsymbol{v}_1 + c\boldsymbol{v}_2, \tag{56}$$

where $c = \cos(\phi)$, $s = \sin(\phi)$, and ϕ is the angle $\boldsymbol{a}$ makes with direction $\boldsymbol{g}_2$. We then have

$$a_1 = s, \quad a_2 = c, \quad a_3 = 0, \quad \zeta_1 = s^2, \quad \zeta_2 = c^2, \quad \zeta_3 = 0. \tag{57}$$

It is clear from (31) that $\varepsilon_{13} = \varepsilon_{23} = 0$.

In this Section, we give results for the case $\sigma_1 = \sigma_3 = 0$ and $\sigma_2 = E_p\tau$ (where τ is a dimensionless variable), where the results will be used to compare with the experimental data of Jin et al. [49] given in Sect. 5. Hence,

$$\bar{\sigma}_1^* = \bar{\sigma}_2^* = -\frac{\tau}{3} = -\gamma = -\frac{\bar{\sigma}_3^*}{2}, \quad h = \tau. \tag{58}$$

The strain components have the forms

$$\varepsilon_{22} = \frac{2}{3}b_1[f_0'(2\gamma) - f_0'(-\gamma)] + b_2 g_0'(\tau) + \frac{1}{3}b_3[2c^2 f_1'(2\gamma) - s^2 f_1(-\gamma)] + \frac{2}{3}b_4 K_2[2c^2 f_2'(2\gamma) - s^2 f_2(-\gamma)] + b_5[g_1(\tau)(2c^2 f_3'(2\gamma) - s^2 f_3(-\gamma)) + K_3 g_1'(\tau)], \tag{59}$$

$$\varepsilon_{11} = \frac{1}{3}b_1[f_0'(-\gamma) - f_0'(2\gamma)] + b_2 g_0'(\tau) + \frac{1}{3}b_3[2s^2 f_1'(-\gamma) - c^2 f_1(2\gamma)] + \frac{2}{3}b_4 K_2[2s^2 f_2'(-\gamma) - c^2 f_2(2\gamma)] + b_5[g_1(\tau)(2s^2 f_3'(-\gamma) - c^2 f_3(2\gamma)) + K_3 g_1'(\tau)], \tag{60}$$

$$\varepsilon_{33} = \frac{1}{3}b_1[f_0'(-\gamma) - f_0'(2\gamma)] + b_2 g_0'(\tau) - \frac{1}{3}b_3[2s^2 f_1'(-\gamma) + c^2 f_1(2\gamma)] - \frac{2}{3}b_4 K_2[2s^2 f_2'(-\gamma) + c^2 f_2(2\gamma)] + b_5[-g_1(\tau)(2s^2 f_3'(-\gamma) + c^2 f_3(2\gamma)) + K_3 g_1'(\tau)], \tag{61}$$

$$\varepsilon_{12} = \frac{cs}{\tau}\{b_3[f_1(2\gamma) - f_1(-\gamma)] + 2b_4 K_2[f_2(2\gamma) - f_2(-\gamma)] + b_5 g_1(\tau)[f_3(2\gamma) - f_3(-\gamma)]\}, \tag{62}$$

where

$$K_2 = s^2 f_2(-\gamma) + c^2 f_2(2\gamma), \quad K_3 = s^2 f_3(-\gamma) + c^2 f_3(2\gamma). \tag{63}$$

5 Modelling of transversely isotropic rock

Complementing the information provided in the Introduction, at the beginning of this Section we review briefly some experimental evidence regarding sources of anisotropy for rock, and we also discuss why nonlinear models are necessary to analyze the behaviour of such material.

In the case of applications to the modelling of transversely isotropic rocks, the source of such transversely isotropic behaviour (and more general anisotropic behaviour) for rocks is multiple. In some cases, such as for sandstones[3], it is possible to clearly see the presence of 'layers', where it is expected that the mechanical behaviour is different in the direction perpendicular to these layers (or lamination depending on the scale) from that in the other directions. In other cases, the source of anisotropy is connected with some particular orientations of the 'grains' or minerals that form rocks, which in some cases have an elongated geometry oriented in some particular directions[4]. The presence of joints, in particular if there is one family of joints oriented in a particular direction (joint set), can also be taken as a reason to consider rock as a transversely isotropic body, and such structures can be incorporated as a part of Π, in the case that the space or distance between each joint is very small in comparison with the overall size of the body being studied[5] [23,31,57]. Note that the presence of cracks and micro-cracks in rock, which may or may not have any particular orientation, may also contribute towards the mechanical behaviour of rock. In compression, some of such cracks can close, whereas in tension they will open, and in both cases, the mechanical behaviour will be different, and it will depend on the stresses; therefore, in general, there is a need for using elaborate models to capture the nonlinear mechanical behaviour of rocks[6]. The presence of cracks and their behaviour in tension and compression is the reason that in the literature, in geology and geomechanics, researchers speak about the 'induced anisotropy' when referring to rock with families of pre-existing cracks [23,24,58,62].

In many applications in geomechanics and geophysics, we may have dissipation of energy, due to, for example, the creation and growth of cracks. In order to simplify our mathematical models, in this Sections we do not consider such dissipation of energy, and we assume that rock is approximately an elastic solid.

In this Section, we compare our theory with the axial tension and compression experiment of Jin et al. [49] on Marcellus shale. We use Eq. (59) to compare our theory with their axial stress–strain experimental data. It is reported in Jin et al. [49] that the ground-state material constants for the tension data are different from those for the compression data. In axial tension, where $\bar{h} > 0$, their ground-state constants are:

$$\begin{aligned} &E_a = 11.50 \pm 1.36\,\text{GPa}\,, \quad E_p = 37.06 \pm 14.18\,\text{GPa}\,, \\ &\nu_{zp} = 0.33 \pm 0.13\,, \quad \nu_p = 0.18 \pm 0.01\,, \quad \mu_a = 6.40 \pm 1.74\,\text{GPa}. \end{aligned} \tag{64}$$

To compare with the axial tension data of Jin et al. [49], we use the ground-state values

$$E_a = 11.50\,\text{GPa}\,, \quad E_p = 25.06\,\text{GPa}\,, \quad \nu_{zp} = 0.33\,, \quad \nu_p = 0.18\,, \quad \mu_a = 6.40\,\text{GPa}\,. \tag{65}$$

These are the same values as those given in (64), taking note that although $E_p = 25.06$ MPa it is within the tolerance range. In axial compression, where $\bar{h} < 0$, Jin's et al. [49] ground-state constants are:

$$\begin{aligned} &E_a = 16.12 \pm 1.29\,\text{GPa}\,, \quad E_p = 37.72 \pm 7.04\,\text{GPa}\,, \\ &\nu_{zp} = 0.35 \pm 0.15\,, \quad \nu_p = 0.25 \pm 0.01\,, \quad \mu_a = 6.87 \pm 1.19\,\text{GPa}. \end{aligned} \tag{66}$$

We use the ground-state values

$$E_a = 13.0\,\text{GPa}\,, \quad E_p = 30.72\,\text{GPa}\,, \quad \nu_{zp} = 0.35\,, \quad \nu_p = 0.25\,, \quad \mu_a = 5.68\,\text{GPa}\,. \tag{67}$$

Except for E_a, all our ground-state values are the same (within the tolerance range) as Jin's et al. [49] values.

We just do a simple ad hoc fitting using the functions

$$f_0(x) = f_1(x) = x^2\,, \quad g_1(x) = f_2(x) = f_3(x) = x, \tag{68}$$

[3] See, for example, [21–23,28,29,53–55] and Figures 1 and 9 of [36].

[4] See Figure 1 of [56], Figures 4–10, 4–13, and 5–14 in [37] and [36].

[5] Other types of discontinuities in rocks that are larger than joints, such as faults, should be incorporated directly in the geometry of the body being studied, and not considered as a part of Π.

[6] See, for example, [23–25,54,58], Figure 11 of [59], [60,61], Figures 2 and 4 of [31], Figure 4 of [63], Figure 5 of [55], Figure 5 of [62], and Figures 8 to 11 in [33].

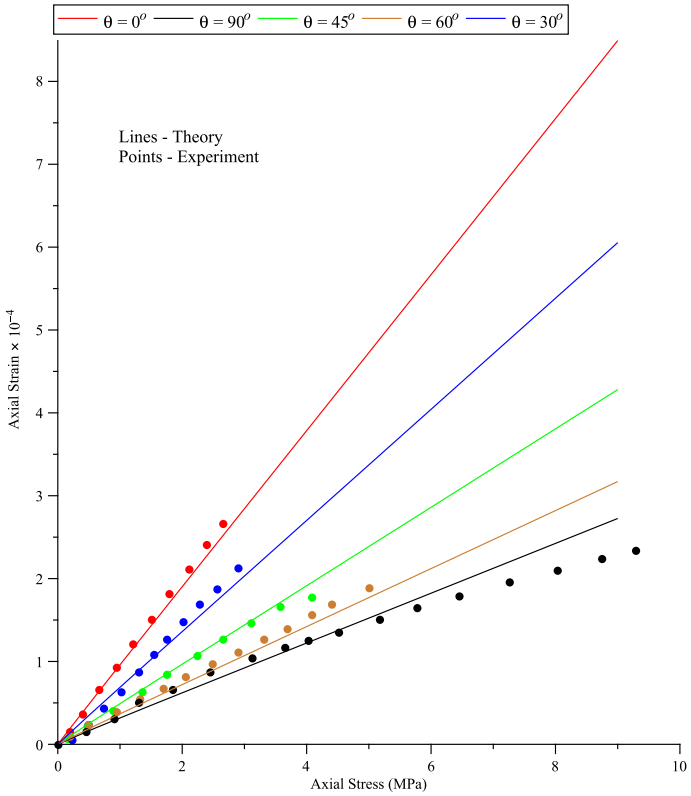

Fig. 1 Strain–stress curves for a uniaxial tension deformation. The points are from the experimental tests of Jin et al., and θ is the angle between the normal vector and the bedding planes with respect to the direction of the load [49]

and

$$g_0'(x) = 2\frac{e^{dx} - 1}{d}\,, \tag{69}$$

where d is a dimensionless parameter. Since the compression/tension behaviour is different, for an ad hoc fitting we use $d = -0.01$ for compression and $d = -2$ for tension. We plot the strain–stress equation (59) when $\boldsymbol{a}$ has the directions described by the angles $\theta = 0°, 30°, 45°, 60°, 90°$ (see Eq. (56)). The tension and compression curves are given in Figs. 1 and 2, respectively. From both Figures, it is clear that our theory captures the behaviour of the experimental data, taking note that some of the curves fit the experiment data quite well.

5.1 Shear and compression of a slab

In this Section, we use the model for rock proposed above to study the behaviour of a slab under shear and compression. Here, we consider the stress distribution to take the form

$$\frac{\boldsymbol{T}}{E_p} = \sigma\, \boldsymbol{g}_1 \otimes \boldsymbol{g}_1 + \tau(\boldsymbol{g}_1 \otimes \boldsymbol{g}_2 + \boldsymbol{g}_2 \otimes \boldsymbol{g}_1) \tag{70}$$

and the preferred direction $\boldsymbol{a}$ given by (56), where σ and τ are dimensionless variables. We then have the principal stresses

$$\hat{\sigma}_1 = \frac{\sigma_1}{E_p} = \frac{1}{2}(\sigma + \sqrt{\sigma^2 + 4\tau^2})\,, \quad \hat{\sigma}_2 = \frac{\sigma_2}{E_p} = \frac{1}{2}(\sigma - \sqrt{\sigma^2 + 4\tau^2})\,, \quad \hat{\sigma}_3 = \frac{\sigma_1}{E_p} = 0\,, \tag{71}$$

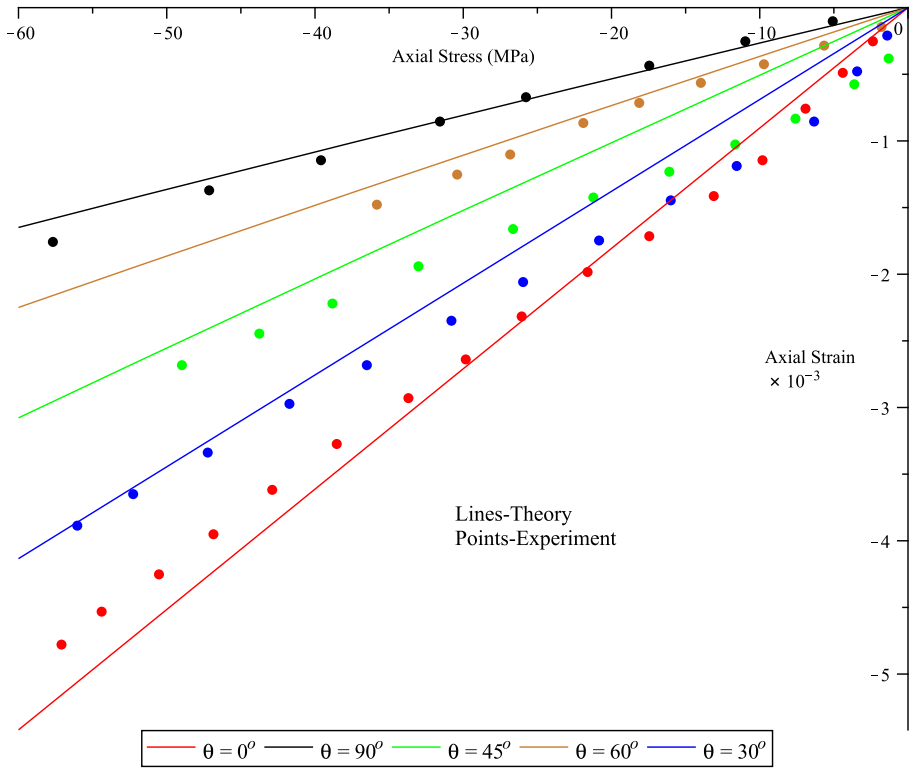

Fig. 2 Strain–stress curves for a uniaxial compression deformation. The points are from the experimental test of Jin et al. [49]

$h = \sigma$, and the eigenvectors

$$\boldsymbol{v}_1 = \frac{1}{\gamma_2}\boldsymbol{g}_1 + \frac{1}{\gamma_1}\boldsymbol{g}_2\,, \quad \boldsymbol{v}_2 = -\frac{1}{\gamma_1}\boldsymbol{g}_1 + \frac{1}{\gamma_2}\boldsymbol{g}_2\,, \quad \boldsymbol{v}_3 = \boldsymbol{g}_3\,, \tag{72}$$

where

$$\frac{1}{\gamma_1} = \frac{\tau}{\sqrt{\hat{\sigma}_1^2 + \tau^2}}\,, \quad \frac{1}{\gamma_2} = \frac{\hat{\sigma}_1}{\sqrt{\hat{\sigma}_1^2 + \tau^2}}\,. \tag{73}$$

For $\boldsymbol{a}$ of the form (56), the spectral components are

$$a_1 = \frac{c}{\gamma_2} + \frac{s}{\gamma_1}\,, \quad a_2 = \frac{-c}{\gamma_1} + \frac{s}{\gamma_2}\,, \quad a_3 = 0, \tag{74}$$

taking note that $\zeta_i = a_i^2$ and

$$\bar{\sigma}_1^* = \frac{\sigma}{6} + \frac{\sqrt{\sigma^2 + 4\tau^2}}{2}\,, \quad \bar{\sigma}_2^* = \frac{\sigma}{6} - \frac{\sqrt{\sigma^2 + 4\tau^2}}{2}\,, \quad \bar{\sigma}_3^* = -\frac{\sigma}{3}\,. \tag{75}$$

The shear strain in the $1-2$ direction, for example, is given by

$$\varepsilon_{12} = \frac{1}{\gamma_1\gamma_2}[\kappa_1 - \kappa_2 + \kappa_3(\gamma_1^2 - \gamma_2^2)]\,, \tag{76}$$

where

$$\kappa_1 = \frac{b_1}{3}[2f_0'(\bar{\sigma}_1^*) - f_0'(\bar{\sigma}_2^*) - f_0'(\bar{\sigma}_3^*)] + b_2 g_0'(\sigma) + \frac{b_3}{3}[2\zeta_1 f_1'(\bar{\sigma}_1^*) - \zeta_2 f_1'(\bar{\sigma}_2^*)] + \frac{2b_4 K_2}{3}[2\zeta_1 f_2'(\bar{\sigma}_1^*) - \zeta_2 f_2'(\bar{\sigma}_2^*)] + b_5\left\{\frac{g_1(\sigma)}{3}[2\zeta_1 f_3'(\bar{\sigma}_1^*) - \zeta_2 f_3'(\bar{\sigma}_2^*)] + K_3 g_1'(\sigma)\right\}, \tag{77}$$

$$\kappa_2 = \frac{b_1}{3}[2f_0'(\bar{\sigma}_2^*) - f_0'(\bar{\sigma}_1^*) - f_0'(\bar{\sigma}_3^*)] + b_2 g_0'(\sigma) + \frac{b_3}{3}[2\zeta_2 f_1'(\bar{\sigma}_2^*) - \zeta_1 f_1'(\bar{\sigma}_1^*)] + \frac{2b_4 K_2}{3}[2\zeta_2 f_2'(\bar{\sigma}_2^*) - \zeta_1 f_2'(\bar{\sigma}_1^*)] + b_5\left\{\frac{g_1(\sigma)}{3}[2\zeta_2 f_3'(\bar{\sigma}_2^*) - \zeta_1 f_3'(\bar{\sigma}_1^*)] + K_3 g_1'(\sigma)\right\}, \tag{78}$$

$$\kappa_3 = \left[b_3\frac{f_1(\bar{\sigma}_1^*) - f_1(\bar{\sigma}_2^*)}{\bar{\sigma}_1^* - \bar{\sigma}_2^*} + 2b_4 K_2\frac{f_2(\bar{\sigma}_1^*) - f_2(\bar{\sigma}_2^*)}{\bar{\sigma}_1^* - \bar{\sigma}_2^*} + b_5 g_1(\sigma)\frac{f_3(\bar{\sigma}_1^*) - f_3(\bar{\sigma}_2^*)}{\bar{\sigma}_1^* - \bar{\sigma}_2^*}\right] a_1 a_2\,, \tag{79}$$

where

$$K_2 = \zeta_1 f_2(\bar{\sigma}_1^*) + \zeta_2 f_2(\bar{\sigma}_2^*)\,, \quad K_3 = \zeta_1 f_3(\bar{\sigma}_1^*) + \zeta_2 f_3(\bar{\sigma}_2^*)\,. \tag{80}$$

In the case of a shear stress without compression, the results are obtained from the above by putting $\sigma = 0$.

In Fig. 3, the shear strain ε_{12} is plotted against the scaled shear stress τ for various values of σ and preferred direction. To depict the Figures, we only consider $h = \sigma \leq 0$, and we use the functions in (68) and (69) with $d = -0.01$. Since $h = \sigma \leq 0$, we use the ground-state constant values given in (67). In Fig. 3(1), we see that larger shear strain is required to maintain the deformation as the magnitude of σ increases. Interestingly, it is indicated in Fig. 3(3) that for the preferred direction, taking $\boldsymbol{a} = \left[\frac{1}{\sqrt{2}}, \frac{1}{\sqrt{2}}, 0\right]^{\mathrm{T}}$, the compression stress causes the shear strain to take a negative value at $\tau = 0$. This is an expected behaviour since at $\tau = 0$ the slab is in pure compression, and since the strain tensor is not coaxial with the Cauchy stress tensor, a shear strain is required to maintain the axial stress field.

6 Conclusions

In this communication, we have presented a constitutive equation for transversely isotropic nonlinear elastic bodies, wherein the linearized strain is a function of the Cauchy stress tensor. In order to show the possible applications of this model, we have applied it to the modelling of a type of transversely isotropic rock. The model captures in a rather simple manner the most significant features of the mechanical behaviour of such material, as indicated in Sect. 5. Rocks are very heterogeneous materials, and even for the same class of rocks, the mechanical behaviour of two samples can be different if they are obtained from two different places. Therefore, it was not the intention of this paper to provide a mathematical model that would fit perfectly a given set of experimental data[7] for a specific type of transversely isotropic rock, but to have a model that can be used in the future to fit data for as many types of transversely isotropic rocks as possible, and also for other types of materials.

In a future work, the behaviour of the P and S waves for transversely isotropic solids will be studied. From the experimental point of view, it is relatively easy to produce small waves travelling across a sample of material under compression for different directions of the preferred direction $\boldsymbol{a}$. The nonlinear constitutive model presented in this paper should be able to capture in particular the dependency of the wave speed in terms of the compressive (time-independent) load (see, for example, [16,66]).

Finally, we note that materials such as rock can show more than one source of anisotropy (see [23,30], Figure 2 of [67] and Figures 4–14 of [37]), and in some cases, it may be necessary to consider two, three or more unit vectors that represent the particular directions where rock is not isotropic. Such cases will be studied in a future work as well.

Acknowledgements The research of R. Bustamante was supported by a grant awarded by FONDECYT (Chile) Under No. 1160030.

[7] As the nonlinear models presented here are new, and only some other few such nonlinear models are available in the literature [16,64,65], most of the experimental data available in the literature are concerned with the determination of the parameters including Young's modulus, shear modulus, etc., that are mostly interesting within the context of the linearized theories.

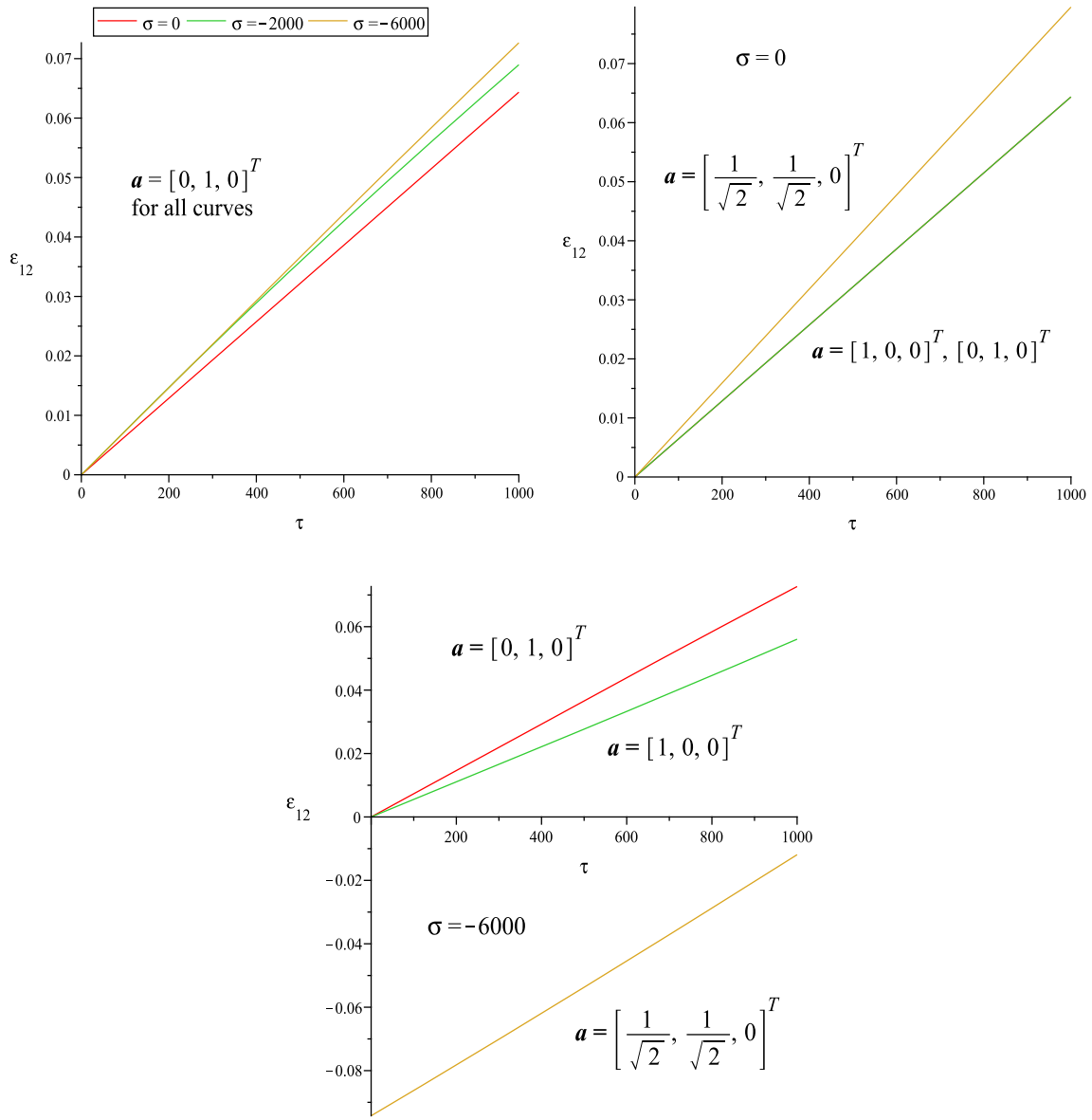

Fig. 3 Shear strain ε_{12} vs scaled shear stress τ for different values of σ and preferred directions $\boldsymbol{a}$

Appendix A

In a general boundary value problem, the values of $\bar{h}$ (or h) themselves depend on the constitutive equation (for details, see [50]), and hence, they cannot be used as a hypothesis to decide what are the appropriate values of the ground-state constants (compression or tension constants) required in a boundary value problem solving process, especially in using the finite element method. To overcome this 'vicious circle', we approximate our proposed discrete constants using the following continuous and differentiable functions:

$$q_{(p)}(h) = \frac{[1 + \operatorname{erf}(\bar{C}h)]}{2}, \quad q_{(n)}(h) = \frac{[1 - \operatorname{erf}(\bar{C}h)]}{2}, \tag{A.1}$$

where erf is the error function and $\bar{C}$ is a very large positive number. Let E_a^t, E_p^t, ν_{zp}^t, ν_p^t, μ_a^t and E_a^c, E_p^c, ν_{zp}^c, ν_p^c, μ_a^c be the tension and compression ground-state values of E_a, E_p, ν_{zp}, ν_p, and μ_a, respectively. We then

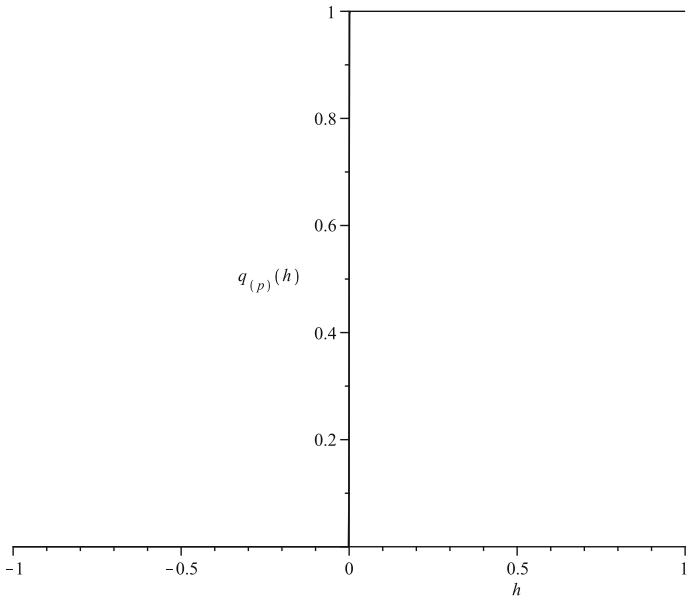

Fig. 4 Plot of $q_{(p)}(h)$, when $\bar{c} = 1000$

use the functions

$$E_a = E_a^t q_{(p)}(h) + E_a^c q_{(n)}(h)\,, \quad E_p = E_p^t q_{(p)}(h) + E_p^c q_{(n)}(h)\,, \quad \nu_{zp} = \nu_{zp}^t q_{(p)}(h) + \nu_{zp}^c q_{(n)}(h)\,,$$
$$\nu_p = \nu_p^t q_{(p)}(h) + \nu_p^c q_{(n)}(h)\,, \quad \mu_a = \mu_a^t q_{(p)}(h) + \mu_a^c q_{(n)}(h)\,. \tag{A.2}$$

For the benefit of the readers, the plot of $q_{(p)}(h)$ with $\bar{C} = 1000$ is given in Fig. 4. It is clear from Fig. 4 that the continuous approximation of the discrete function is not accurate, when the argument h (say) of the function is very close to zero. The accuracy of the continuous function could be improved by using a value of $\bar{C}$ larger than 1000. For practical purposes, we let the value of the derivatives of $q_{(p)}$ and $q_{(n)}$ be zero.

References

1. Rajagopal, K.R.: On implicit constitutive theories. Appl. Math. **48**, 279–319 (2003)
2. Rajagopal, K.R.: The elasticity of elasticity. Z. Angew. Math. Phys. **58**, 309–317 (2007)
3. Rajagopal, K.R.: Conspectus of concepts of elasticity. Math. Mech. Solids **16**, 536–562 (2011)
4. Rajagopal, K.R., Srinivasa, A.R.: On the response of non-dissipative solids. Proc. R. Soc. A **463**, 357–367 (2007)
5. Rajagopal, K.R., Srinivasa, A.R.: On a class of non-dissipative materials that are not hyperelastic. Proc. R. Soc. A **465**, 493–500 (2009)
6. Rajagopal, K.R., Srinivasa, A.R.: Inelastic response of solids described by implicit constitutive relations with nonlinear small strain elastic response. Int. J. Plast. **71**, 1–9 (2015)
7. Rajagopal, K.R., Srinivasa, A.R.: An implicit three-dimensional model for describing the inelastic response of solids undergoing finite deformation. Z. Angew. Math. Phys. **67**, 86 (2016)
8. Bustamante, R.: Some topics on a new class of elastic bodies. Proc. R. Soc. A **465**, 1377–1392 (2009)
9. Bustamante, R., Rajagopal, K.R.: A note on plane strain and plane stress problems for a new class of elastic bodies. Math. Mech. Solids **15**, 229–238 (2010)
10. Bustamante, R., Rajagopal, K.R.: A note on some new classes of constitutive relations for elastic bodies. IMA J. Appl. Math. **80**, 1287–1299 (2015)
11. Rajagopal, K.R.: Non-linear elastic bodies exhibiting limiting small strain. Math. Mech. Solids **16**, 122–139 (2011)
12. Rajagopal, K.R.: On the nonlinear elastic response of bodies on the small strain range. Acta Mech. **225**, 1545–1553 (2014)
13. Grasley, Z., El-Helou, R., D'Amborsia, M., Mokarem, D., Moen, C., Rajagopal, K.R.: Model of infinitesimal nonlinear elastic response of concrete subjected to uniaxial compression. J. Eng. Mech. **141**, 04015008 (2015)
14. Devendiran, V.K., Sandeep, R.K., Kannan, K., Rajagopal, K.R.: A thermodynamically consistent constitutive equation for describing the response exhibited by several alloys and the study of a meaningful physical problem. Int. J. Solids Struct. **108**, 1–10 (2017)
15. Kulvait, V., Málek, J., Rajagopal, K.R.: Modelling gum metal and other newly developed titanium alloys within a new class of constitutive relations for elastic bodies. Arch. Mech. **69**, 223–241 (2017)

16. Bustamante, R., Rajagopal, K.R.: A nonlinear model for describing the mechanical behaviour of rock. Acta Mech. **229**, 251–272 (2018)
17. Gou, K., Mallikarjuna, M., Rajagopal, K.R., Walton, J.R.: Modeling fracture in the context of a strain-limiting theory of elasticity: A single plane-strain crack. Int. J. Eng. Sci. **88**, 73–82 (2015)
18. Kulvait, V., Málek, J., Rajagopal, K.R.: Anti-plane stress state of a plate with a V-notch for a new class of elastic solids. Int. J. Fract. **179**, 59–73 (2013)
19. Bustamante, R., Rajagopal, K.R.: Study of a new class of nonlinear inextensible elastic body. Z. Angew. Math. Phys. **66**, 3663–3677 (2015)
20. Bustamante, R., Rajagopal, K.R.: A review of implicit constitutive theories to describe the response of elastic bodies. In: Merodio, J., Ogden, R.W. (eds.) Constitutive Modelling of Solid Continua, pp. 187–230. Springer, Switzerland (2019)
21. Abbas, H.A., Mohamed, Z., Yasir, S.F.: A review of methods, techniques and approaches on investigation of rock anisotropy. AIP Conf. Proc. **2020**, 020012 (2018)
22. Al-Harthi, A.A.: Effect of planar structures on the anisotropy of Ranyah sandstone Saudi Arabia. Eng. Geol. **50**, 49–57 (1998)
23. Amadei, B.: Importance of anisotropy when estimating and measuring in situ stresses in rock. Int. J. Rock. Mech. Min. Sci. & Geomech. Abstr. **33**, 293–325 (1996)
24. Attenwel, P.B., Sandford, M.R.: Intrinsic shear strength of a brittle, anisotropic rock-III. Textural interpretation of failure. Int. J. Rock Mech. Min. Sci. & Geomech. Abstr. **11**, 439–451 (1974)
25. Barla, G.: Rock anisotropy. Theory and laboratory testing. In: Müller, L. (ed.) Rock Mechanics, pp. 131–169. Springer, Berlin (1972)
26. Chen, C.S., Pan, E., Amadei, B.: Determination of deformability and tensile strength of anisotropic rock using Brazilian tests. Int. J. Rock Mech. Min. Sci. **35**, 43–61 (1998)
27. Cobbold, P.R., Cosgrove, J.W., Summers, J.M.: Development of internal structures in deformed anisotropic rocks. Tectonophysics **12**, 23–53 (1971)
28. Gholami, R., Rasouli, V.: Mechanical and elastic properties of transversely isotropic slate. Rock Mech. Rock Eng. **47**, 1763–1773 (2014)
29. Heng, S., Guo, Y., Yang, C., Daemen, J.J.K., Li, Z.: Experimental and theoretical study of the anisotropic properties of shale. Int. J. Rock Mech. Min. Sci. **74**, 58–68 (2015)
30. Homand, F., Morel, E., Henry, J.P., Cuxac, P., Hammade, E.: Characterization of the moduli of elasticity of an isotropic rock using dynamic and static methods. Int. J. Rock Mech. Min. Sci. Geomech. Abstr. **30**, 527–535 (1993)
31. Kulhawy, F.H.: Stress deformation properties of rock and rock discontinuities. Eng. Geol. **9**, 327–350 (1975)
32. Lo, T.W., Coyner, K.B., Toksöz, M.N.: Experimental determination of elastic anisotropy of Berea sandstone, Chicopee shale, and Chelmsford granite. Geophysics **51**, 164–171 (1986)
33. Nasseri, M.H.B., Rao, K.S., Ramamurthy, T.: Anisotropic strength and deformational behavior of Himalayan schists. Int. J. Rock Mech. Min. Sci. **40**, 3–23 (2003)
34. Niandou, H.: Étude du comportement rhéologique et modélisation de L' argilite de Tournemire. Applications à la stabilité d' ouvrages souterrains. Doctorate Thesis, Université des Sciences et Technologies de Lille (1994)
35. Shea, W.T., Kronenberg, A.K.: Strength and anisotropy of foliated rocks with varied mica contents. J. Struct. Geol. **15**, 1097–1121 (1993)
36. Song, I., Suh, M., Woo, Y.K., Hao, T.: Determination of the elastic modulus set of foliated rocks from ultrasonic velocity measurements. Eng. Geol. **72**, 293–308 (2004)
37. Turner, F.J., Weiss, L.E.: Structural Analysis of Metamorphic Tectonics. McGraw Hill, New York (1963)
38. Wang, Y., Li, C.H.: Investigation of the P- and S-wave velocity of a Longmaxi formation shale by real-time ultrasonic and mechanical experiments under uniaxial deformation. J. Pet. Sci. Eng. **158**, 253–267 (2017)
39. Wu, Y., Li, X., He, J., Zheng, B.: Mechanical properties of Longmaxi black organic-rich shale samples from south China under uniaxial and triaxial compression states. Energies **9**, 1088 (2016)
40. Shariff, M.H.B.M.: Nonlinear transversely isotropic elastic solids: An alternative representation. Q. J. Mech. Appl. Math. **61**, 129–149 (2008)
41. Truesdell, C.A., Toupin, R.: The Classical Theories. In: Flügge, S. (ed.) Handbuch der Physik, vol. III/I, pp. 226–902. Springer, Berlin (1960)
42. Gokulnath, C., Saravanan, U., Rajagopal, K.R.: Representations for implicit constitutive relations describing non-dissipative response of isotropic materials. Z. Angew. Math. Phys. **68**, 129 (2017)
43. Truesdell, C.A., Noll, W.: The Non-linear Field Theories of Mechanics, 3rd ed. (Antmann S.S. ed). Springer, Heidelberg (2004)
44. Xiao, H., Chen, L.S.: Hencky's logarithmic strain and dual stress-strain and strain-stress relations in isotropic finite hyperelasticity. Int. J. Solid Struct. **40**, 1455–1463 (2003)
45. Xiao, H., Bruhns, O.T., Meyers, A.: Explicit dual stress-strain and strain-stress relations of incompressible isotropic hyperelastic solids via deviatoric Hencky strain and Cauchy stress. Acta Mech. **168**, 21–33 (2004)
46. Srinivasa, A.R.: On a class of Gibbs potential-based nonlinear elastic models with small strains. Acta Mech. **226**, 571–583 (2015)
47. Průša, V., Rajagopal, K.R., Tůma, K.: Gibbs free energy based representation formula within the context of implicit constitutive relations for elastic solids. Int. J. Nonlinear Mech. **121**, 103433 (2020)
48. Blume, J.A.: On the form of the inverted stress-strain law for isotropic hyperelastic solids. Int. J. Nonlinear Mech. **27**, 413–421 (1992)
49. Jin, W., Lia, Z., Jin, W., Hambletona, C., Cusatisa, G.: Anisotropic elastic, strength, and fracture properties of Marcellus shale. Int. J. Rock Mech. Min. Sci. **109**, 124–137 (2018)
50. Shariff, M.H.B.M.: On the spectral constitutive modelling of transversely isotropic soft tissue: physical invariants. Int. J. Eng. Sci. **120**, 199–219 (2017)

51. Shariff, M.H.B.M.: Anisotropic separable free energy functions for elastic and non-elastic solids. Acta Mech. **227**, 3213–3237 (2016)
52. Shariff, M.H.B.M.: Spectral derivatives in continuum mechanics. Q. J. Mech. Appl. Math. **70**, 479–476 (2017)
53. Niandou, H., Shao, J.F., Henry, J.P., Fourmaintraux, D.: Laboratory investigation of the mechanical behaviour of Tournemire shale. Int. J. Rock Mech. Min. Sci. **34**, 3–16 (1997)
54. Chenevert, M.E., Gattin, C.: Mechanical anisotropies of laminated sedimentary rocks. Soc. Pet. Eng. J. **5**, 67–77 (1965)
55. McLamore, R., Gray, K.E.: The mechanical behavior of anisotropic sedimentary rocks. J. Eng. Ind. **89**, 62–73 (1967)
56. Saroglou, H., Tsiambaos, G.: A modified Hoek-Brown failure criterion for anisotropic intact rock. Int. J. Rock Mech. Min. Sci. **45**, 223–234 (2008)
57. Singh, B.: Continuum characterization of jointed rock masses. Int. J. Rock Mech. Min. Sci. Geomech. Abstr. **10**, 311–335 (1973)
58. Douglass, P.M., Voight, B.: Anisotropy of granites: a reflection of microscopic fabric. Géotechnique **19**, 376–398 (1969)
59. Handin, J., Hager, R.V.: Experimental deformation of sedimentary rocks under confining pressure: test at room temperature on dry samples. B. Am. Ass. Petroleum Geol. **41**, 1–50 (1957)
60. Jizba, D.L.: Mechanical and acoustical properties of sandstones and shales. PhD. Thesis, Standford University (1991)
61. Johnson, P.A., Rasolofosaon, P.N.J.: Manifestation of nonlinear elasticity in rock: convincing evidence over large frequency and strain intervals from laboratory studies. Nonlinear Process. Geophys. **3**, 77–88 (1996)
62. Morgenstern, N.R., Tamuy Phukan, A.L.: Non-linear stress-strain relations for a homogeneous sandstone. Int. J. Rock Mech. Min. Sci. **6**, 127–142 (1969)
63. Li, Z., Xu, G., Huang, P., Zhao, X., Fu, Y.: Experimental study on anisotropic properties of Silurian silty slates. Geotech. Geol. Eng. **35**, 1755–1766 (2017)
64. Guyer, R.A., Johnson, P.A.: Nonlinear Mesoscopic Elasticity: The Complex Behaviour of Granular Media Including Rocks and Soil. Wiley, Weinheim (2009)
65. Lyakhowsky, V., Hamiel, Y., Ampuero, J.P., Ben-Zion, Y.: Nonlinear damage rehology and wave resonance in rocks. Geophysics **178**, 910–920 (2009)
66. Shariff, M.H.B.M. R. Bustamante R.: A consistent isotropic spectral constitutive equation: The infinitesimal strain depends nonlinearly on the stress. Appl. Eng. Sci. https://doi.org/10.1016/j.apples.2020.100007
67. Motra, H.B., Hager, J., Ismail, A., Wutlke, F., Rabbel, W., Köhn, D., Thorwart, M., Simonetta, C., Costantine, N.: Determining the influence of pressure and temperature on the elastic constants of anisotropic rock samples using ultrasonic wave techniques. J. Appl. Geophys. **259**, 715–730 (2018)